



## Sustainable approaches for dye removal using enzymatic hydrolysis residue of corncob as an adsorbent

Guilong Yan<sup>a,b,c,d,\*</sup>, Yuzhen Zhou<sup>a,c,d</sup>, Xinyi Zhao<sup>a</sup>, Jianguo Wu<sup>a,c,d</sup>, Ci Jin<sup>a,c,d</sup>, Liqin Zhao<sup>a,c,d</sup>, Wei Wang<sup>a,c,d</sup>, Ying Chen<sup>a</sup>, Xiaoya Yao<sup>a</sup>

<sup>a</sup>School of Life Sciences, Huaiyin Normal University, Huai'an 223300, China, Tel.: +8651783525993; emails: ygllong@163.com (G. Yan), zyz@hytc.edu.cn (Y. Zhou), 1948598902@qq.com (X. Zhao), jgwu\_hytc@163.com (J. Wu), jinci@hytc.edu.cn (C. Jin), zhaoliqin@hytc.edu.cn (L. Zhao), weiwang2599@hytc.edu.cn (W. Wang), 1661065889@qq.com (Y. Chen), 1296857225@qq.com (X. Yao)

<sup>b</sup>Jiangsu Key Laboratory for Food Safety and Nutrition Function Evaluation, Huaiyin Normal University, Huai'an 223300, China

<sup>c</sup>Jiangsu Key Laboratory for Eco-Agricultural Biotechnology around Hongze Lake, Huaiyin Normal University, Huai'an 223300, China

<sup>d</sup>Jiangsu Collaborative Innovation Center of Regional Modern Agriculture & Environmental Protection, Huaiyin Normal University, Huai'an, China

Received 8 January 2023; Accepted 17 June 2023

### ABSTRACT

In this study, the potential of enzymatic hydrolysis residue of corncob (EHRC), an intrinsic byproduct of biorefinery, as dye adsorbent was surveyed. The chemical and structural analysis indicated that EHRC and raw corncob had numerous active functional groups and a large, rough adsorption surface. These properties, more prominent in EHRC, underlined the material's efficiency in dye adsorption. EHRC and raw corncob were more favorable for the adsorption of methylene blue (MB) than methyl orange. The adsorption capacities of both EHRC and raw corncob increased with increasing initial dye concentration, and adsorption occurred rapidly. The adsorption capacity of EHRC did not change much when the solution pH was greater than the pH at point zero charge ( $\text{pH}_{\text{pzc}}$  3.78). The process modelling demonstrated that adsorption of MB onto EHRC well fitted by the pseudo-second-order and Langmuir isotherm models. The adsorption was a spontaneous exothermic reaction based on thermodynamic analysis. These results showed that EHRC could be used as an efficient and cheap adsorbent.

**Keywords:** Adsorption; Dyes; Enzymatic hydrolysis residue of corncob (EHRC); Isotherms; Kinetics; Thermodynamics

### 1. Introduction

The progressing of modern industry inflicted severe environmental pollution, especially contamination of freshwater, causing increasingly serious economic and social problems [1,2]. Among various pollutants in wastewater, one of most important pollutants is dye [3,4]. Dyes are extensively used in the textile, printing, cosmetics, paper, and food industries [5,6], and often directly discharged into water [7], causing harm to plant, animal and human health [4,7]. Therefore, it is necessary to remove

these harmful dyes from polluted water. Several methods for removing dyes from wastewaters have been developed, such as chemical oxidation [8], adsorption [9], flocculation [10], membrane filtration [11], and biodegradation [12]. Among the various methods, adsorption is considered the best option because of its operational simplicity and high efficiency [13]. Recently, researchers focus more on finding novel adsorbent with high adsorption capacity, and some excellent adsorbents were developed, such as polymeric nanocomposites [14], metal-organic frameworks [15] and modified activated carbons [16], etc. However, the cost of

\* Corresponding author.

these adsorbents' applications in wastewater treatment were extremely high. Thus, many researchers have searched for natural, cheap, and highly efficient adsorbents, and have found some candidates, that include agricultural waste, natural clays, and industry by-products [17–19].

Biorefinery using lignocellulosic biomass is a potentially sustainable solution for future fossil depletion and environmental pollution [20]. However, due to the complexity and recalcitrance of lignocellulose, it is difficult to convert lignocellulosic biomass into biofuel and value-added products economically [21]. Therefore, greater efforts should be made to lower the costs. Recent studies have investigated the conversion of lignocellulose using the processes of pretreatment, enzymatic hydrolysis, and fermentation, but the enzymatic hydrolysis residue (EHR) has rarely been studied and utilized. Therefore, the effective utilization of the residue could reduce not only the cost of biorefinery, but also environmental pollution. EHR might be an effective adsorbent used to remove the dye from wastewater, because EHR has a large surface area and many cavities after enzymatic hydrolysis. In addition, EHR does not require regeneration and is readily available.

The purpose of this study is to assess the enzymatic hydrolysis residue of corncob (EHRC) as an efficient and cost-effective adsorbent for dye adsorption from aqueous solutions. And EHRC was characterized by composition analysis, Fourier-transform infrared spectroscopy (FTIR), and scanning electron microscopy (SEM). The effects of adsorption conditions on adsorption capacity and dye removal were explored. In addition, the adsorption kinetics, adsorption isotherm, and thermodynamics were investigated.

## 2. Materials and methods

### 2.1. Preparation and characterization of the adsorbent

The sun-dried corncobs were milled and screened to a mesh size of 60. Then, the pulverized corncobs were rinsed and dried at 60°C for 48 h.

EHRC were prepared according to the previous studies [22]. First, the corncob was pretreated with a deep eutectic solvent (DES). The DES was synthesized by mixing oxalic acid and choline chloride (molar ratio 1:1). At 80°C, 80 g corncob and 800 g DES were mixed and stirred. After 1 h, the slurry was vacuum filtered after being combined with 800 mL of absolute ethanol. The residues were further washed twice with 800 mL of ethanol and deionized water. The obtained residues were subjected to enzymatic hydrolysis. The solids loading was 5% (w/v), and hydrolysis was conducted in 50 mM citrate buffer (pH 4.8) at 50°C, the enzyme loading was 15 mg protein/g solid CTec2 and 7.5 mg protein/g solid HTec2 (Novozymes, Bagsværd, Denmark). After hydrolysis for 72 h, the mixture was vacuum-filtrated, and the enzymatic hydrolysis residue was collected and dried via lyophilization before being utilized.

The compositional analysis was measured with the NREL protocols [23] and our previous report [22]. Attenuated total reflection-FTIR (ATR-FTIR) was attained with a spectral resolution of 4 cm<sup>-1</sup> for 32 scans between 4,000 and 400 cm<sup>-1</sup> on a Thermo Nicolet iS50 FTIR spectrometer [22]. The raw corncob and EHRC were

gold-sputtered and then observed using a Quanta FEG450 SEM (Oxford Instruments, Netherlands) under vacuum using a 10 kV accelerating voltage [24].

### 2.2. Batch adsorption studies

The experiments were performed by mixing 300 mg adsorbent with 30 mL of dye solution in a 50 mL glass vial at the desired concentration and temperature, then shaking the mixture at 60 rpm on a TR-02U rotary shaker (Crystal Technology & Industries, China). The initial concentrations of methylene blue (MB) and methyl orange (MO) ranged from 10 to 200 mg/L, and from 10 to 120 mg/L, respectively. The temperatures were 20°C, 30°C, 40°C, and 50°C, respectively. The dye solutions were sampled at set time intervals (from 10 to 50 min), and the dye concentrations of the samples were measured using a UV-Vis spectrophotometer at 664 nm for MB and 464 nm for MO. All experiments were performed three times.

The adsorption capacity of the adsorbent at a given time ( $q_t$ ) and equilibrium ( $q_e$ ) were calculated according to Eqs. (1) and (2). The percentage of dye removal was calculated using Eq. (3).

$$q_t = \frac{(C_0 - C_t)V}{m} \quad (1)$$

$$q_e = \frac{(C_0 - C_e)V}{m} \quad (2)$$

$$\text{Dye removal}(\%) = \frac{C_0 - C_e}{C_0} \times 100\% \quad (3)$$

where  $C_0$  is the initial concentration of dyes (mg/L), the concentrations of dyes at time  $t$  and equilibrium are presented by  $C_t$  (mg/L) and  $C_e$  (mg/L), respectively;  $V$  (L) represents the volume of dye solution, and  $m$  is the amount of adsorbent (g).

The effect of initial solution pH was evaluated in the range from 1.0 to 11.0 with a MB concentration of 80 mg/L at 30°C. The pH at point zero charge ( $\text{pH}_{\text{PZC}}$ ) of EHRC was determined by the method reported by Ofomaja and Ho [25]. The change ( $\Delta\text{pH}$ ) between the initial and final pH values of the dye solution was plotted against the initial pH, the  $\text{pH}_{\text{PZC}}$  is determined by the point at which the intercept of the plot is zero.

### 2.3. Kinetic models

To investigate the mechanism of adsorption, the experimental data were used to fit with the pseudo-first-order [Eq. (4)] and pseudo-second-order [Eq. (5)] [26].

$$q_t = q_1(1 - e^{-k_1 t}) \quad (4)$$

$$q_t = \frac{q_2^2 k_2 t}{1 + q_2 k_2 t} \quad (5)$$

where  $q_1$  and  $q_2$  are the theoretical adsorption capacities (mg/g), the rate constants of the two models are presented by  $k_1$  (min<sup>-1</sup>) and  $k_2$  (g/mg·min), respectively.

#### 2.4. Adsorption isotherm analysis

To understand the interaction behavior between adsorbate and adsorbent, Langmuir [Eq. (6)] and Freundlich isotherm equations [Eq. (7)] were extensively used models [17,26].

$$q_e = \frac{Q_m K_L C_e}{1 + K_L C_e} \quad (6)$$

$$q_e = K_F C_e^{1/n} \quad (7)$$

The type of adsorption was determined by the separation factor ( $R_L$ ), which is the essential characteristics of Langmuir model and is defined as Eq. (8) [27].

$$R_L = \frac{1}{1 + K_L C_0} \quad (8)$$

#### 2.5. Thermodynamic parameters

The Gibbs free energy change ( $\Delta G$ ) was determined by Eq. (9) [28,29]:

$$\Delta G = -RT \ln \frac{q_e}{C_e} \quad (9)$$

where  $R$  and  $T$  represent the universal gas constant (8.314 J/mol·K) and temperature (K), respectively.

The enthalpy change ( $\Delta H$ ) and entropy change ( $\Delta S$ ) were determined by Eq. (10) [28,29]:

$$\Delta G = \Delta H - T\Delta S \quad (10)$$

### 3. Results and discussion

#### 3.1. Chemical and structural features of raw corncob and EHRC

The chemical compositions of the raw corncob and EHRC was evaluated by measuring the material major component, cellulose, hemicellulose and lignin. As shown in Fig. 1a, the raw corncob contained 31.62% cellulose, 28.75% hemicellulose and 16.31% lignin, whereas, the EHRC was composed of 45.46% cellulose, 10.96% hemicellulose, and 23.1% lignin. These components are known to contain numerous polar groups, suggesting that their high contents in the analysed materials may favor the adsorption of ionic dyes.

The FTIR spectra of the raw corncob and EHRC are shown in Fig. 1b. The broad bands at 3,320 and 2,885  $\text{cm}^{-1}$  are responsible for the O–H stretching vibration of cellulose and lignin [30]. These bands showed significantly higher intensity for EHRC compared to raw corncob, confirming the data of chemical composition analysis which indicated that EHRC contains more cellulose and lignin. The C=C aromatic skeletal vibration were assigned to the bands 1,621 and 1,510  $\text{cm}^{-1}$  [31]. The COOH groups stretching in aromatic compounds were assigned to the absorption band at 1,602  $\text{cm}^{-1}$  [30]. The bands at 1,313 and 1,105  $\text{cm}^{-1}$  can be associated with the C–O stretching of syringyl nuclei and the C–O linkage in lignin or cellulose [32]. Other bands associated with C–O–C vibration were observed at around 1,158 and 1,037  $\text{cm}^{-1}$  [31,33]. According to the results of FTIR, the major surface groups of EHRC are polar groups, such as –OH, –COC–, –C=C–, –COOH, and –CO–. These functional

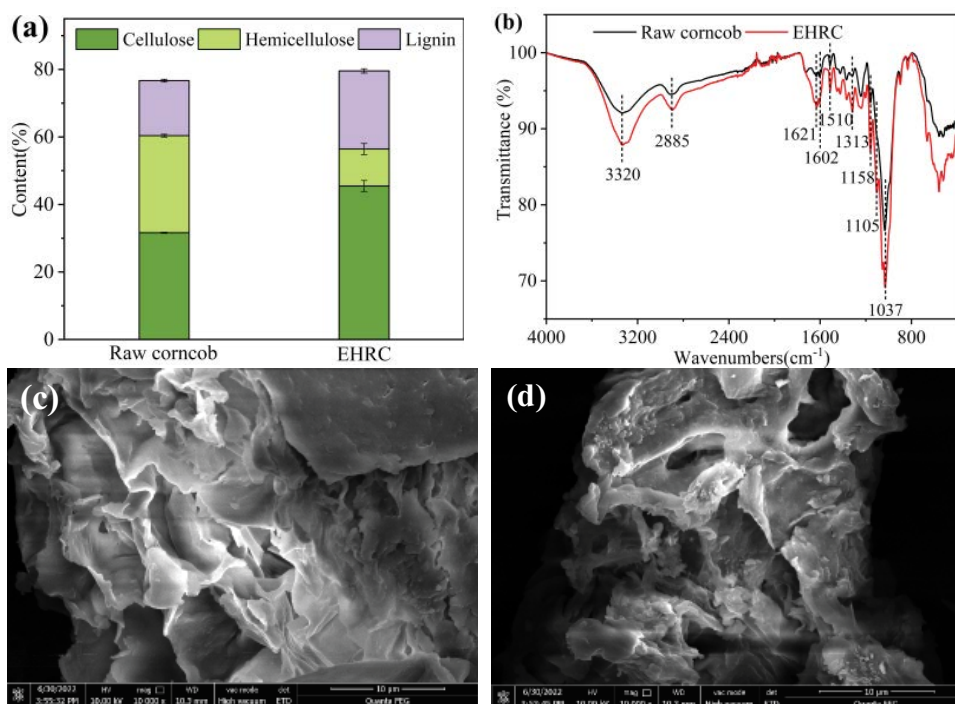


Fig. 1. Composition of raw corncob and EHRC (a), Fourier-transform infrared spectra of raw corncob and EHRC (b), scanning electron microscopy of raw corncob (c) and EHRC (d) (magnification, 10,000 $\times$ ).

groups can adsorb cationic dyes by electrostatic interaction [32], but they are not considered to be efficient adsorbents for anionic dyes. In addition, FTIR analysis showed that the EHRC had a stronger peak intensity than the raw corncob at the above bands, indicating that EHRC contains more functional groups than raw corncob. This observation well agrees with the assumption that EHRC may be a better adsorbent for cationic dye removal.

The surface structures of raw corncob and EHRC were surveyed by SEM. The surface morphological changes are depicted in Fig. 1c and d, the surface of raw corncob is smooth (Fig. 1c), while the surface of EHRC is rough and has many cavities (Fig. 1d). These differences may be beneficial for dye adsorption.

### 3.2. Effect of initial dye concentration

The efficiency of adsorption and removal of MB and MO from aqueous solutions using EHRC and raw corncob were studied by varying the initial dye concentrations. As shown in Fig. 2, the adsorption capacities of EHRC and raw corncob almost proportionally increased with the increase in the initial dye concentrations. When the initial MB concentrations were increased from 10 to 200 mg/L, the adsorption capacity at equilibrium increased from 0.98 to 17.87 mg/g for EHRC and from 0.97 to 17.62 mg/g for raw corncob, respectively. The adsorption capacity of EHRC was slightly higher than that of raw corncob, which is consistent with the FTIR analysis results. However, the experiments with MO showed quite different adsorption behavior. When the initial MO concentrations varied from 10 to 120 mg/L, the adsorption capacities for EHRC and raw corncob increased only from 0.46 to 4.27 mg/g and from 0.41 to 3.53 mg/g, respectively. It was found that the adsorption capacity of EHRC or raw corncob for MO was much lower than that for MB, this result was also confirmed by FTIR analysis. These results also indicate that the initial dye concentration has a positive impact on the adsorption capacities of EHRC and raw corncob, which may be due to a stronger mass transfer driving force at a higher initial concentration [34].

The data presented in Fig. 2 also describes the dye removal at different dye concentrations in the aqueous solution. It can be noticed that the dye removal decreased as the dye concentration increased. With the increase of MB concentration from 10 to 200 mg/L, the dye removal of EHRC

decreased from 97.53% to 89.37%, and that of raw corncob decreased from 96.76% to 88.11%. Ratnamala et al. [34] obtained similar results using sawdust as an adsorbent. The dye removal of EHRC decreased from 46.00% to 35.72%, and that of raw corncob decreased from 41.42% to 29.38%, with an increase in MO concentration from 10 to 120 mg/L.

These results suggested that EHRC or raw corncob was unsuitable for anionic dye removal, such as MO. Similar results were reported by Janbooranapinij et al. [35]. Therefore, the adsorption behavior of MO has not been studied further.

### 3.3. Effects of initial solution pH and point of zero charge

According to previous studies [36], the  $pH_{PZC}$  of an adsorbent plays an important role in determining its adsorption affinity to the adsorbate. As shown in Fig. 3a, the  $pH_{PZC}$  of EHRC was found at pH 3.78. The result indicated that the surface of EHRC will possess negative charge and favor adsorption of cationic dye when the solution pH is above the  $pH_{PZC}$  [34]. The effect of solution pH on the adsorption capacity of EHRC is shown in Fig. 3b. It was found that the adsorption capacity of EHRC increased from 6.73 to 7.85 mg/g as the pH increase from 1 to 5, and the adsorption capacity changed little when the pH increased from 5.0 to 11.0. Jawad et al. [37] also reported similar result that the adsorption capacity did not change much when the solution pH was greater than the  $pH_{PZC}$  of EHRC. And in the subsequent experiments, natural MB solution ( $\sim$ pH 5.6) [38] was used to investigate kinetics of the adsorption process with the aim to get details on the rate and mechanism of adsorption.

### 3.4. Adsorption kinetics

The study of adsorption kinetics can provide much information about the rate and mechanism of adsorption. Fig. 4 shows the simulation plots of the pseudo-first-order and pseudo-second-order kinetic models, and the model parameters are presented in Table 1. As shown in Fig. 4, MB uptake was rapid for the first 10 min at different dye concentrations, and then became slower until the adsorption reached equilibrium. The adsorption at the initial stage was rapid because a large number of vacant sites were available on the adsorbent [39]. This may be one of the advantages

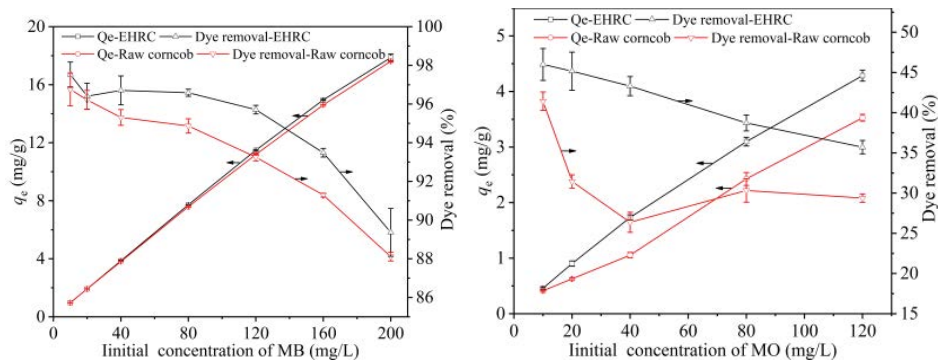


Fig. 2. Effect of initial dye concentration on the amount of adsorption and dye removal.

of EHRC as an adsorbent, as it can reach equilibrium in a shorter time. Compared with other adsorbents, such as chemically modified rice husk [40], and *Butea monosperma* leaf [41], their equilibrium was reached over 30 min.

Based on Fig. 3 and Table 1, it can be seen that the correlation factors of the pseudo-second-order model were close to 1, which was relatively higher than those of the pseudo-first-order model. In addition, the calculated  $q_2$  of the pseudo-second-order model showed good compliance with the experimental  $q_e$ . Compared with  $q_2$ . These

results indicate that the pseudo-second-order model best describes the adsorption of MB onto EHRC.

### 3.5. Adsorption isotherms

Curve fitting to the experimental data using the Langmuir and Freundlich isotherm model is represented in Fig. 5, and the adsorption isotherm constants are listed in Table 2. According to Table 2, the Langmuir model fit the experimental data of MB sorption on EHRC better because

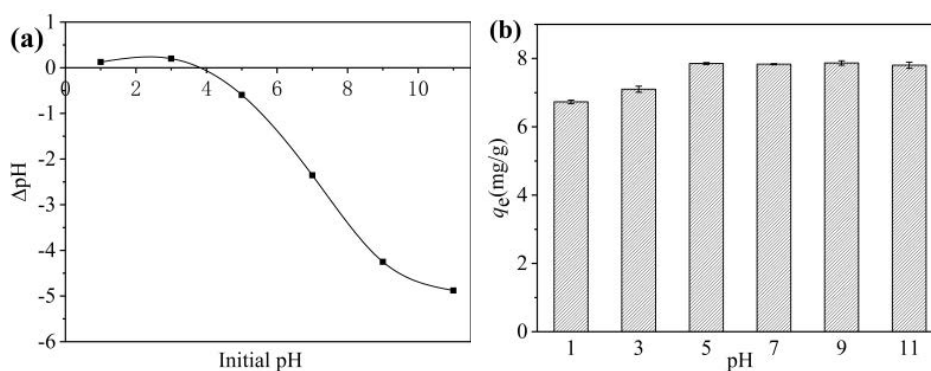


Fig. 3.  $pH_{PZC}$  of EHRC (a), and effect of pH on the methylene blue adsorption (b).

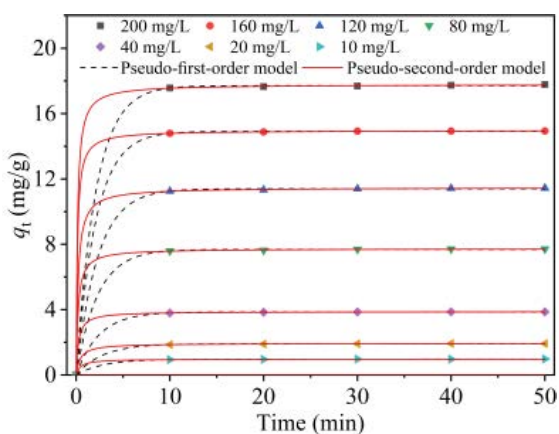


Fig. 4. Plot of kinetic models for the adsorption of methylene blue onto EHRC.

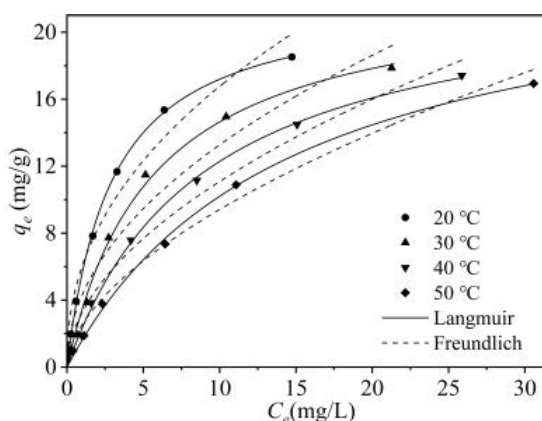


Fig. 5. Equilibrium isotherms for the adsorption of methylene blue onto EHRC.

Table 1  
Constants and correlation coefficients of kinetic models for the adsorption of methylene blue onto EHRC

Initial methylene blue concentration (mg/L)	Experimental $q_e$ (mg/g)	Pseudo-first-order kinetic model			Pseudo-second-order kinetic model		
		$q_1$ (mg/g)	$k_1$ (min <sup>-1</sup> )	$R^2$	$q_2$ (mg/g)	$k_2$ (g/mg·min)	$R^2$
200	17.8734	17.7130	0.4797	0.9997	17.7932	0.4129	≈1
160	14.9576	14.9178	0.4787	0.9999	14.9776	0.5336	≈1
120	11.4857	11.4027	0.4356	0.9998	11.4804	0.4200	≈1
80	7.72692	7.6820	0.4415	0.9998	7.7340	0.6375	≈1
40	3.86834	3.8564	0.4146	0.9999	3.88851	1.0937	≈1
20	1.92815	1.9114	0.3588	0.9996	1.9373	1.2091	≈1
10	0.97529	0.9664	0.3570	0.9995	0.9805	2.2542	≈1

Table 2  
Parameters of adsorption isotherms for the adsorption of methylene blue onto EHRC

Temperature	Langmuir isotherm model			Freundlich isotherm model		
	$Q_m$ (mg/g)	$K_L$ (L/mg)	$R^2$	$K_F$ (mg <sup>1-1/n</sup> ·L <sup>1/n</sup> /g)	$n$	$R^2$
20°C	22.2585	0.3397	0.9991	6.0421	2.2559	0.9615
30°C	22.8121	0.1804	0.9958	4.3198	2.0448	0.9486
40°C	23.2460	0.1121	0.9985	3.2764	1.8889	0.9792
50°C	24.8551	0.0697	0.9984	2.5430	1.7588	0.9864

Table 3  
Thermodynamics parameter for adsorption of methylene blue onto EHRC

$\Delta H$ (kJ/mol)	$\Delta S$ (J/(mol·K))	$\Delta G$ (kJ/mol)			
		293.15 K	303.15 K	313.15 K	323.15 K
-35.03	-104.80	-4.65	-2.72	-2.30	-1.29

it had higher correlation factor values, indicating that the adsorption was monolayer adsorption [17,42]. Furthermore, the  $K_L$  values of the Langmuir model were greater than zero, implying that the  $R_L$  values were in the range of 0–1, this indicated that the adsorption of MB onto EHRC was favorable [4].

### 3.6. Adsorption thermodynamics

The thermodynamics of MB adsorption with EHRC were investigated by varying the temperature at 40 mg/L of the initial dye concentration. The thermodynamic parameters are summarized in Table 3. The negative value of  $\Delta H$  suggested that the adsorption was exothermic [43], which is consistent with the experimental results that higher adsorption capacity is correlated with lower temperature [13]. In addition, the negative value of  $\Delta S$  revealed that the adsorption of MB onto EHRC decreased the degree of freedom at the solid–liquid interface [43]. Moreover, the results suggested that the adsorption was spontaneous, because the values of  $\Delta G$  were negative.

## 4. Conclusions

In this study, the biorefinery byproduct of EHRC has been explored as an eco-friendly dye adsorbent. The following conclusions were obtained:

- The surface of EHRC is large and has sufficient functional groups, which are beneficial for dye adsorption.
- EHRC and raw corncob were more favorable for the adsorption of MB (cationic dye) than MO (anionic dye), because of their negatively charged surfaces.
- The adsorption capacity of both EHRC and raw corncob showed positive correlation with initial dye concentration. The adsorption capacity of EHRC remains constant at pH level higher than the  $pH_{PZC}$  (pH = 3.78).
- The adsorption of MB on EHRC follows the pseudo-second-order and Langmuir isotherm models.

The kinetic and thermodynamic analysis also suggested that the adsorption was a rapid spontaneous exothermic process.

- The EHRC could be considered as a novel, efficient and inexpensive adsorbent for a range of industrial dyes.

## Acknowledgments

This work was supported by the Major Basic Research Project of the Natural Science Foundation of the Jiangsu Higher Education Institutions (18KJA550001).

## References

- [1] Q. Zhang, Y. Cheng, C. Fang, J. Shi, J. Chen, H. Han, Functionalized waste cellulose with metal-organic-frameworks as the adsorbent with adjustable pore size: ultralight, effective, and selective removal of organic dyes, *J. Solid State Chem.*, 302 (2021) 122361, doi: 10.1016/j.jssc.2021.122361.
- [2] C. Long, Z. Jiang, J. Shangguan, T. Qing, P. Zhang, B. Feng, Applications of carbon dots in environmental pollution control: a review, *Chem. Eng. J.*, 406 (2021) 126848, doi: 10.1016/j.cej.2020.126848.
- [3] S. Shi, M.A. Gondal, K. Shen, M.A. Ali, Q. Xu, X. Chang, Batch and column adsorption of dye contaminants using a low-cost sand adsorbent, *Res. Chem. Intermed.*, 41 (2015) 6999–7013.
- [4] M.R. Islam, M.G. Mostafa, Adsorption kinetics, isotherms and thermodynamic studies of methyl blue in textile dye effluent on natural clay adsorbent, *Sustainable Water Resour. Manage.*, 8 (2022) 52, doi: 10.1007/s40899-022-00640-1.
- [5] S. Benkhaya, S. M'Rabet, A. El Harfi, A review on classifications, recent synthesis and applications of textile dyes, *Inorg. Chem. Commun.*, 115 (2020) 107891, doi: 10.1016/j.inoche.2020.107891.
- [6] V. Selvaraj, T.S. Karthika, C. Mansiya, M. Alagar, An over review on recently developed techniques, mechanisms and intermediate involved in the advanced azo dye degradation for industrial applications, *J. Mol. Struct.*, 1224 (2021) 129195, doi: 10.1016/j.molstruc.2020.129195.
- [7] S. Akhouairi, H. Ouachtak, A.A. Addi, A. Jada, J. Douch, Natural sawdust as adsorbent for the Eriochrome Black T dye removal from aqueous solution, *Water Air Soil Pollut.*, 230 (2019) 181, doi: 10.1007/s11270-019-4234-6.
- [8] G.A. Ismail, H. Sakai, Review on effect of different type of dyes on advanced oxidation processes (AOPs) for textile color removal, *Chemosphere*, 291 (2022) 132906, doi: 10.1016/j.chemosphere.2021.132906.
- [9] J. Wu, T. Zhang, C. Chen, L. Feng, X. Su, L. Zhou, Y. Chen, A. Xia, X. Wang, Spent substrate of *Ganoderma lucidum* as a new bio-adsorbent for adsorption of three typical dyes, *Bioresour. Technol.*, 266 (2018) 134–138.
- [10] G. Han, C. Liang, T. Chung, M. Weber, C. Staudt, S. Maletzko, Combination of forward osmosis (FO) process with coagulation/flocculation (CF) for potential treatment of textile wastewater, *Water Res.*, 91 (2016) 361–370.

- [11] J. Lin, W. Ye, M.-C. Baltaru, Y.P. Tang, N.J. Bernstein, P. Gao, S. Balta, M. Vlad, A. Volodin, A. Sotto, P. Luis, A.L. Zydney, B. Van der Bruggen, Tight ultrafiltration membranes for enhanced separation of dyes and  $\text{Na}_2\text{SO}_4$  during textile wastewater treatment, *J. Membr. Sci.*, 514 (2016) 217–228.
- [12] K.T. Rainert, H.C.A. Nunes, M.J. Gonçalves, C.V. Helm, L.B.B. Tavares, Decolorization of the synthetic dye Remazol Brilliant Blue Reactive (RBBR) by *Ganoderma lucidum* on bio-adsorbent of the solid bleached sulfate paperboard coated with polyethylene terephthalate, *J. Environ. Chem. Eng.*, 9 (2021) 104990, doi: 10.1016/j.jece.2020.104990.
- [13] S. Zhang, M. Yang, L. Qian, C. Hou, R. Tang, J. Yang, X. Wang, Design and preparation of a cellulose-based adsorbent modified by imidazolium ionic liquid functional groups and their studies on anionic dye adsorption, *Cellulose*, 25 (2018) 3557–3569.
- [14] G. Sarojini, P. Kannan, N. Rajamohan, M. Rajasimman, D.N. Vo, Dyes removal from water using polymeric nanocomposites: a review, *Environ. Chem. Lett.*, 21 (2023) 1029–1058.
- [15] Y. Zhao, Y. Hang Chai, L. Ding, S. Wang, Y. Wang, L. Ma, B. Zhao, A stable N-containing heterocyclic carboxylic acid ligand Co-MOF for photoelectric performance and anionic dyes adsorption, *Arabian J. Chem.*, 16 (2023) 104878, doi: 10.1016/j.arabjc.2023.104878.
- [16] M. Sultana, M.H. Rownok, M. Sabrin, M.H. Rahaman, S.M.N. Alam, A review on experimental chemically modified activated carbon to enhance dye and heavy metals adsorption, *Cleaner Eng. Technol.*, 6 (2022) 100382, doi: 10.1016/j.clet.2021.100382.
- [17] J.O. Paul Nayagam, K. Prasanna, Utilization of shell-based agricultural waste adsorbents for removing dyes: a review, *Chemosphere*, 291 (2022) 132737, doi: 10.1016/j.chemosphere.2021.132737.
- [18] I. Anastopoulos, M. Karamesouti, A.C. Mitropoulos, G.Z. Kyzas, A review for coffee adsorbents, *J. Mol. Liq.*, 229 (2017) 555–565.
- [19] S. Mor, M.K. Chhavi, K.K. Sushil, K. Ravindra, Assessment of hydrothermally modified fly ash for the treatment of methylene blue dye in the textile industry wastewater, *Environ. Dev. Sustainability*, 20 (2018) 625–639.
- [20] M.M. Demeke, F. Dumortier, Y. Li, T. Broeckx, M.R. Foulquié-Moreno, J.M. Thevelein, Combining inhibitor tolerance and D-xylose fermentation in industrial *Saccharomyces cerevisiae* for efficient lignocellulose-based bioethanol production, *Biotechnol. Biofuels*, 6 (2013) 120, doi: 10.1186/1754-6834-6-120.
- [21] A. Patel, A.R. Shah, Integrated lignocellulosic biorefinery: Gateway for production of second generation ethanol and value added products, *J. Bioresour. Bioprod.*, 6 (2021) 108–128.
- [22] G. Yan, Y. Zhou, L. Zhao, W. Wang, Y. Yang, X. Zhao, Y. Chen, X. Yao, Recycling of deep eutectic solvent for sustainable and efficient pretreatment of corncob, *Ind. Crops Prod.*, 183 (2022) 115005, doi: 10.1016/j.indcrop.2022.115005.
- [23] A. Sluiter, B. Hames, R. Ruiz, C. Scarlata, J. Sluiter, D. Templeton, D. Crocker, Determination of structural carbohydrates and lignin in biomass, *Natl. Renewable Energy Lab.*, 1617 (2008) 1–16.
- [24] J.M. Jabar, Y.A. Odusote, K.A. Alabi, I.B. Ahmed, Kinetics and mechanisms of Congo red dye removal from aqueous solution using activated *Moringa oleifera* seed coat as adsorbent, *Appl. Water Sci.*, 10 (2020) 136, doi: 10.1007/s13201-020-01221-3.
- [25] A.E. Ofomaja, Y.-S. Ho, Effect of temperatures and pH on methyl violet biosorption by *Mansonia* wood sawdust, *Bioprocess Technol. Rep.*, 99 (2008) 5411–5417.
- [26] A.H. Jawad, A.S. Abdulhameed, L.D. Wilson, S.S.A. Syed-Hassan, Z.A. AlOthman, M.R. Khan, High surface area and mesoporous activated carbon from KOH-activated dragon fruit peels for methylene blue dye adsorption: optimization and mechanism study, *J. Chem. Eng.*, 32 (2021) 281–290.
- [27] A.L. Ahmad, C.Y. Chan, S.R. Abd Shukur, M.D. Mashitah, Adsorption kinetics and thermodynamics of  $\beta$ -carotene on silica-based adsorbent, *Chem. Eng. J.*, 148 (2009) 378–384.
- [28] T. Unugul, F.U. Nigiz, Preparation and characterization of an active carbon adsorbent from waste mandarin peel and determination of adsorption behavior on removal of synthetic dye solutions, *Water Air Soil Pollut.*, 231 (2020) 538, doi: 10.1007/s11270-020-04903-5.
- [29] F. Kiani Ghaleh sardi, M. Behpour, Z. Ramezani, S. Masoum, Simultaneous removal of Basic Blue41 and Basic Red46 dyes in binary aqueous systems via activated carbon from palm bio-waste: optimization by central composite design, equilibrium, kinetic, and thermodynamic studies, *Environ. Technol. Innovation*, 24 (2021) 102039, doi: 10.1016/j.eti.2021.102039.
- [30] O.A. Fakayode, E.A.A. Aboagarib, D. Yan, M. Li, H. Wahia, A.T. Mustapha, C. Zhou, H. Ma, Novel two-pot approach ultrasonication and deep eutectic solvent pretreatments for watermelon rind delignification: parametric screening and optimization via response surface methodology, *Energy*, 203 (2020) 117872, doi: 10.1016/j.energy.2020.117872.
- [31] Q. Qing, Z. Ma, P. Chen, Q. Zhang, D. Chen, L. Wang, Y. Zhang, Two-step liquefaction process of lignocellulose in acetone/ $\text{H}_2\text{O}$  medium for non-enzymatic sugar production, *Biomass Convers. Biorefin.*, (2022), doi: 10.1007/s13399-021-02202-5.
- [32] M.P. da Rosa, A.V. Igansi, S.F. Lütke, T.R. Sant’Anna Cadaval, A.C.R. do Santos, A.P. de Oliveira Lopes Inacio, L.A. de Almeida Pinto, P.H. Beck, A new approach to convert rice husk waste in a quick and efficient adsorbent to remove cationic dye from water, *J. Environ. Chem. Eng.*, 7 (2019) 103504, doi: 10.1016/j.jece.2019.103504.
- [33] Y. Akköz, R. Coşkun, A. Delibaş, Preparation and characterization of sulphonated bio-adsorbent from waste hawthorn kernel for dye (MB) removal, *J. Mol. Liq.*, 287 (2019) 110988, doi: 10.1016/j.molliq.2019.110988.
- [34] G.M. Ratnamala, U.B. Deshannavar, S. Munyal, K. Tashildar, S. Patil, A. Shinde, Adsorption of reactive blue dye from aqueous solutions using sawdust as adsorbent: optimization, kinetic, and equilibrium studies, *Arabian J. Sci. Eng.*, 41 (2016) 333–344.
- [35] K. Janbooranapini, A. Yimponpipatpol, N. Ngamthanacom, G. Panomsuwan, Conversion of industrial carpet waste into adsorbent materials for organic dye removal from water, *Cleaner Eng. Technol.*, 4 (2021) 100150, doi: 10.1016/j.clet.2021.100150.
- [36] M. Kosmulski, The pH-dependent surface charging and the points of zero charge, *J. Colloid Interface Sci.*, 253 (2002) 77–87.
- [37] A.H. Jawad, R. Razuan, J.N. Appaturi, L.D. Wilson, Adsorption and mechanism study for methylene blue dye removal with carbonized watermelon (*Citrullus lanatus*) rind prepared via one-step liquid phase  $\text{H}_2\text{SO}_4$  activation, *Surf. Interfaces*, 16 (2019) 76–84.
- [38] T.L. Kua, M.R.R. Kooh, M.K. Dahri, N.A.H.M. Zaidi, Y. Lu, L.B.L. Lim, Aquatic plant, *Ipomoea aquatica*, as a potential low-cost adsorbent for the effective removal of toxic methyl violet 2B dye, *Appl. Water Sci.*, 10 (2020) 1–13.
- [39] J. Feng, J. Zhang, W. Song, J. Liu, Z. Hu, B. Bao, An environmental-friendly magnetic bio-adsorbent for high-efficiency Pb(II) removal: preparation, characterization and its adsorption performance, *Ecotoxicol. Environ. Saf.*, 203 (2020) 111002, doi: 10.1016/j.ecoenv.2020.111002.
- [40] C. Namasivayam, R.T. Yamuna, Removal of Congo red from aqueous solutions by biogas waste slurry, *J. Chem. Technol. Biotechnol.*, 53 (2007) 153–157.
- [41] M. Das, A.K. Samal, N. Mehar, *Butea monosperma* leaf as an adsorbent of methylene blue: recovery of the dye and reuse of the adsorbent, *Int. J. Environ. Sci. Technol.*, 17 (2020) 2105–2112.
- [42] P. Arabkhani, A. Asfaram, The potential application of bio-based ceramic/organic xerogel derived from the plant sources: a new green adsorbent for removal of antibiotics from pharmaceutical wastewater, *J. Hazard. Mater.*, 429 (2022) 128289, doi: 10.1016/j.jhazmat.2022.128289.
- [43] A. Onder, P. Ilgin, H. Ozay, O. Ozay, Preparation of composite hydrogels containing fly ash as low-cost adsorbent material and its use in dye adsorption, *Int. J. Environ. Sci. Technol.*, 19 (2022) 7031–7048.